MODELLING A PM MACHINE WITH SHIELDING CYLINDER

H. Polinder, M.J. Hoeijmakers

Delft University of Technology, The Netherlands

1 INTRODUCTION

1.1 Objective

This paper originates from a research project, the aim of which is the development of a high-speed, high-efficiency generator system. It consists of a permanent-magnet generator with surface-mounted magnets and a six-pulse rectifier, because these components enable high efficiency, high reliability, high power density, and high speed. The generator system can be applied in series-hybrid vehicles (figure 1), aircraft, vessels, and total energy units.

The objective of this paper is to model the permanent-magnet generator of the generator system. The generator has a copper shielding cylinder surrounding the rotor (figure 2) to avoid excessive eddy-current losses in the permanent magnets and the probably solid rotor iron [1]. The model is used to determine the losses in the shielding cylinder. These losses are important because high rotor losses may result in demagnetization of the magnets.

Analytic methods are used to obtain direct relations between the dimensions of the machine and the parameters in the model, which is useful when the machine design is optimized.

For the accurate analytic calculation of the rotor losses, the magnetic field must be calculated including space harmonics and two-dimensionally. Therefore, both the radial and the tangential component of the magnetic field are calculated. Further, the current waveforms must be determined. Therefore, the model consists of voltage equations that can be combined with a rectifier model.

In [1, 2, 3], the magnetic field in the air-gap of a PM machine with a retaining or shielding cylinder is also calculated two-dimensionally. However, the models in these papers are quite complicated, so that it is difficult to use them to calculate current waveforms. Often, stylized current waveforms are used.

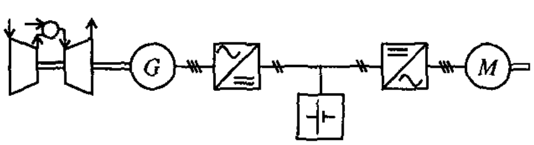

Figure 1: The drive system of a series-hybrid vehicle, consisting of gas turbine, PM generator, rectifier, accumulator, inverter and motor.

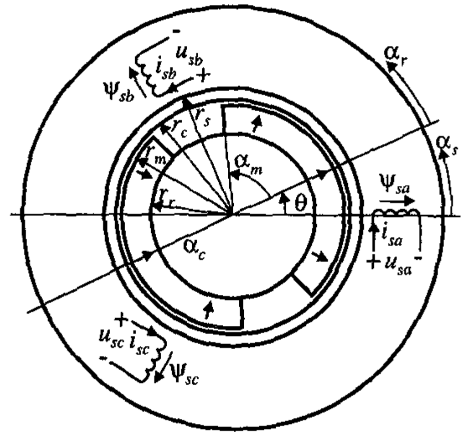

Figure 2: Section of a 2-pole PM machine with shielding cylinder.

The additional value of this paper is that it introduces a model based on the two-dimensional calculation of the magnetic field which is also suitable for the determination of the voltage and current waveforms.

1.2 Outline of the paper

The paper starts with the two-dimensional calculation of the magnetic field in the air gap of the machine. Next, the voltage equations are derived, which are verified by means of locked-rotor tests. Subsequently, the losses in the shielding cylinder of a rectifier-loaded PM machine are calculated. Finally, conclusions are drawn.

1.3 Assumptions

The derivations in this paper are based on the following assumptions.

The magnetic permeability of the stator and the rotor iron is assumed to be infinite.

Eddy currents in the stator and the rotor iron and in the magnets are assumed to be negligible.

The stator and the rotor surface are assumed to be cylindrical; effects of stator slots are neglected.

The machine is assumed to be symmetrical, so that for all quantities $x(\alpha_s+\pi/p) = -x(\alpha_s)$ is valid, where p is the number of pole pairs.

The shielding cylinder is assumed to be so thin that it can be replaced by a surface current density and that

skin effect is negligible. It is possible to incorportate skin effect by solving the Helmholz equation [2, 3]. However, this has not been done in this paper because this would complicate the derivation of voltage equations considerably and because the cylinder is very thin; a fibre bandage is as a retainment sleeve.
End effects are assumed to be negligible. Therefore,
* the magnetic field is two-dimensional: it has no axial component,
* the current density in the shielding cylinder only flows in axial direction, and
* the resistance and the leakage inductance of the end connections of the shielding cylinder are neglected.

It is possible to calculate both the axial and the tangential component of the current density in the shielding cylinder. In [4], is done for linear machines. However, for the frequencies of the harmonics in this paper, it is reasonable to assume that the current density only flows in the axial direction because the magnetic Reynold's number [4] is rather large.

2 CALCULATION OF THE MAGNETIC FIELD

2.1 Calculation method

This subsection gives the differential equation for the calculation of the magnetic field and the boundary conditions. These equations are only given because the derivations have been described in [5, 6]. For more elaborate derivations is referred to standard books as [7].
The magnetic field is calculated using the differential equation for the magnetic vector potential $\vec{A}$ that follows from Maxwell's equations for magnetoquasistatic fields:

$$\nabla^2\vec{A} = \begin{cases} \mu_0\nabla\times\vec{M}_p & \text{in the magnets} \\ 0 & \text{in the air spaces} \end{cases} \qquad (1)$$

where $\vec{M}_p$ is the permanent magnetization.
From the magnetic vector potential, the magnetic flux density $\vec{B}$ follows with

$$\vec{B} = \nabla\times\vec{A} \qquad (2)$$

To solve the equations for the magnetic field, we also need boundary conditions at the boundaries between different regions. The magnetic flux continuity condition prescribes that the magnetic flux density normal to a surface between medium a and medium b is continuous:

$$\vec{n}\cdot(\vec{B}^a-\vec{B}^b) = 0 \qquad (3)$$

Ampère's continuity condition prescribes that there is a jump in the tangential component of the magnetic field strength $\vec{H}$ as one passes through a surface current density K between medium a and medium b:

$$\vec{n}\times(\vec{H}^a-\vec{H}^b) = K \qquad (4)$$

Therefore, to calculate the magnetic field, we need descriptions of the permanent magnetization of the magnets and of the stator and the cylinder surface current densities, which are given in the next subsections.

2.2 The permanent magnets

If the permanent magnetization of the magnet pole arcs only has a radial component given by $M_{pr}=M_{pm}r_r/r$, it can be written as a Fourier series [5, 6]:

$$M_{pr}(r,\alpha_r) = \sum_{k=1,3,5,..}^{\infty} \hat{M}_{p,k}\frac{r_r}{r}\cos(kp\alpha_r) \; ; \qquad \hat{M}_{p,k} = \frac{4}{k\pi}M_{pm}\sin(kp\alpha_m) \qquad (5)$$

where α_m is half the magnet pole arc (see figure 2).

2.3 The surface current density of the stator

The current in the stator slots is replaced by a surface current density K_s on the stator surface at the place of the slot openings. The conductor density n_{sa} (the number of conductors per radian, as introduced in [8]) of phase a is a function of the stator coordinate α_s:

$$n_{sa}(\alpha_s) = \sum_{k=1,3,5,..}^{\infty} \tfrac{1}{2}N_{s,k}\sin(kp\alpha_s) \qquad (6)$$

In this equation, $N_{s,k}$ is the number of turns of the kth space harmonic of the conductor density, which is related to the actual number of turns N by

$$N_{s,k} = \frac{4}{\pi}k_{w,k}N\sin(\tfrac{1}{2}k\pi) \qquad (7)$$

where $k_{w,k}$ is the winding factor for the kth space harmonic of the actual winding.
The conductor densities of phases b and c are equal to the conductor density of phase a, except for an angular shift of their axes. Using this, the surface current density of a three-phase stator can be expressed as

$$K_s(\alpha_s) = \sum_{k=1,3,5,..}^{\infty} \frac{N_{s,k}}{2r_s}\cdot \left\{i_{sa}\sin(kp\alpha_s)+i_{sb}\sin(k(p\alpha_s-\tfrac{2}{3}\pi))+i_{sc}\sin(k(p\alpha_s-\tfrac{4}{3}\pi))\right\} \qquad (8)$$

2.4 The surface current density of the cylinder

Under the assumptions mentioned, the surface current density of the shielding cylinder can be written as:

$$K_c(\alpha_r) = \sum_{k=1,3,5,..}^{\infty} K_{c,k}(\alpha_r) \; ; \qquad K_{c,k}(\alpha_r) = \hat{K}_{c,k}\sin(kp(\alpha_r-\gamma_k)) \qquad (9)$$

This surface current density can also be considered as a series of currents in a series of sinusoidally-distributed windings. This will appear useful when the voltage equations representing the shielding cylinder and the equivalent circuit are derived. For the kth space harmonic, the winding distributions of the two sinusoidally distributed windings are given by

$$\begin{cases} n_{cd,k}(\alpha_r) = \tfrac{1}{2}N_{c,k}\sin(kp\alpha_r) \\ n_{cq,k}(\alpha_r) = \tfrac{1}{2}N_{c,k}\sin(kp\alpha_r-\tfrac{1}{2}\pi) \end{cases} \qquad (10)$$

Subscripts d and q are used for the rotor-connected two-phase dq-system. The current in the direct- and the quadrature-axis winding are called $i_{cd,k}$ and $i_{cq,k}$ respectively. With this, the kth space harmonic of the surface current density can be written as

$$K_{c,k}(\alpha_r) = \frac{N_{c,k}}{2r_c}\left\{i_{cd,k}\sin(kp\alpha_r) + i_{cq,k}\sin(kp\alpha_r - \tfrac{1}{2}\pi)\right\} \quad (11)$$

To obtain the surface current density of (9), the currents must be given by

$$\begin{bmatrix} i_{cd,k} \\ i_{cq,k} \end{bmatrix} = \frac{2r_c\hat{K}_{c,k}}{N_{c,k}}\begin{bmatrix}\cos(kp\gamma_k) \\ \sin(kp\gamma_k)\end{bmatrix} \quad (12)$$

2.5 The magnetic field

The differential equation (1) is solved using the boundary conditions with the stator and the cylinder surface current densities and the description of the permanent magnetization. The result is only given for the region between the stator and the shielding cylinder, because this result is used in the derivation of the voltage equations:

$$A_z(r,\alpha) = \sum_{k=1,3,5,..}^{\infty} \frac{(r^{2kp}+r_s^{2kp})(r_m^{2kp}-r_r^{2kp})}{2(r_s^{2kp}-r_r^{2kp})r_m^{kp}r^{kp}}\frac{r_r\mu_0\hat{M}_{p,k}}{kp}\sin(kp\alpha_r)$$
$$+\frac{(r^{2kp}+r_r^{2kp})r_s^{kp}}{(r_s^{2kp}-r_r^{2kp})r^{kp}}\frac{\mu_0 N_{s,k}}{2kp}\cdot \quad (13)$$
$$\left\{i_{sa}\sin(kp\alpha_s)+i_{sb}\sin(k(p\alpha_s-\tfrac{2}{3}\pi))+i_{sc}\sin(k(p\alpha_s-\tfrac{4}{3}\pi))\right\}$$
$$+\frac{(r^{2kp}+r_s^{2kp})(r_c^{2kp}+r_r^{2kp})}{2(r_s^{2kp}-r_r^{2kp})r_c^{kp}r^{kp}}\frac{\mu_0 N_{c,k}}{2kp}\cdot$$
$$\left\{i_{cd,k}\sin(kp\alpha_r)+i_{cq,k}\sin(kp\alpha_r-\tfrac{1}{2}\pi)\right\}$$

3 THE VOLTAGE EQUATIONS

This section describes how the stator and the cylinder voltage equations are derived. These equations are transformed to the stator-connected $\alpha\beta$-system to eliminate the dependance of the rotor position. To save space, only the resulting equations are written out.

3.1 The stator voltage equation

The stator voltages are given by

$$\begin{bmatrix} u_{sa} \\ u_{sb} \\ u_{sc}\end{bmatrix} = R_s\begin{bmatrix} i_{sa} \\ i_{sb} \\ i_{sc}\end{bmatrix} + \frac{\mathrm{d}}{\mathrm{d}t}\begin{bmatrix}\psi_{soa}+\psi_{sma} \\ \psi_{sob}+\psi_{smb} \\ \psi_{soc}+\psi_{smc}\end{bmatrix} \quad (14)$$

where R_s is the stator resistance. The flux linkages in this equation are separated into two contributions. The first contribution is the flux linkage due to end winding and slot leakage fields, which can be written as

$$\begin{bmatrix}\psi_{soa} \\ \psi_{sob} \\ \psi_{soc}\end{bmatrix} = \begin{bmatrix} L_{soa} & M_{soab} & M_{soab} \\ M_{soab} & L_{soa} & M_{soab} \\ M_{soab} & M_{soab} & L_{soa}\end{bmatrix}\begin{bmatrix} i_{sa} \\ i_{sb} \\ i_{sc}\end{bmatrix} \quad (15)$$

thanks to the symmetry of the stator.
The other contribution is the flux linkage due to the air-gap field, which can be calculated in the following way. The flux linkage of an arbitrary winding is related to the magnetic vector potential by using (2) in the general equation for the flux linkage, which is further simplified by using Stokes' integral theorem [7]:

$$\psi = \iint_S \vec{B}\cdot\mathrm{d}\vec{a} = \iint_S \nabla\times\vec{A}\cdot\mathrm{d}\vec{a} = \oint_C \vec{A}\cdot\mathrm{d}\vec{s} \quad (16)$$

With this, the flux linkage of a full-pitch turn at the stator surface at stator coordinate α_s is calculated as

$$\psi_t(\alpha_s) = l_s(A_z(r_s,\alpha_s)-A_z(r_s,\alpha_s+\frac{\pi}{p})) = 2l_sA_z(r_s,\alpha_s) \quad (17)$$

where l_s is the stack length of the machine. The second step in this equation is valid because of the symmetry of the machine. From this expression, the flux linkage of stator phase a is obtained by integration:

$$\psi_{sma} = p\int_0^{\pi/p} n_{sa}(\alpha_s)\psi_t(\alpha_s)\mathrm{d}\alpha_s = 2pl_s\int_0^{\pi/p} n_{sa}(\alpha_s)A_z(r_s,\alpha_s)\mathrm{d}\alpha_s \quad (18)$$

The magnetic vector potential of (13) is written as a function of the stator coordinate α_s by substituting $\alpha_r=\alpha_s-\theta$, where θ is the rotor position angle (figure 2) and substituted in (18). For the other phases, the same is done. The result transformed in subsection 3.3.

3.2 Voltage equations for the shielding cylinder

The current density $\vec{J}$ in the shielding cylinder is calculated by means of the second of Maxwell's equations. Using (2) in this equation results in

$$\nabla\times\vec{E} = -\frac{\partial\vec{B}}{\partial t} = -\frac{\partial\nabla\times\vec{A}}{\partial t} \quad (19)$$

where $\vec{E}$ is the electric field strength.
It appears that a satisfying solution of this equation is

$$\vec{E} = -\frac{\partial\vec{A}}{\partial t} \quad (20)$$

In this equation, it is taken that $\vec{E}=\rho_c\vec{J}$, where ρ_c is the resistivity of the shielding cylinder. Further, two assumptions mentioned earlier are taken, namely that end effects and skin effect are negligible. The current density in the shielding cylinder is then given by

$$J_z(\alpha_r) = -\frac{1}{\rho_c}\frac{\partial A_z}{\partial t} \quad (21)$$

From this, the surface current density is calculated as

$$K_c(\alpha_r) = -\frac{\delta_c}{\rho_c}\frac{\partial A_z}{\partial t} \tag{22}$$

where δ_c is the thickness of the shielding cylinder.
In this equation, the magnetic vector potential of (13) is substituted. In the same way as in subsection 2.4, this surface current density can be written as a series of currents in a series of sinusoidally distributed windings. Another way of calculating the currents in the sinusoidally-distributed windings representing the shielding cylinder is using the voltage equations of the short-circuited windings:

$$\begin{bmatrix}0\\0\end{bmatrix} = R_{c,k}\begin{bmatrix}i_{cd,k}\\i_{cq,k}\end{bmatrix} + \frac{\mathrm{d}}{\mathrm{d}t}\begin{bmatrix}\Psi_{cd,k}\\\Psi_{cq,k}\end{bmatrix} \tag{23}$$

The flux linkages can be calculated in the same way as the stator flux linkages ((16) to (18)). Comparison of the result with the result of (22) shows that the cylinder can indeed be modelled as a series of short-circuited sinusoidally-distributed windings. It also results in a value of the resistance $R_{c,k}$.

3.3 Transformation to the $\alpha\beta$-system

The stator quantities are transformed to the stator-connected $\alpha\beta$-system using the Clarke-transformation:

$$\begin{bmatrix}i_{s\alpha}\\i_{s\beta}\end{bmatrix} = C_{23}\begin{bmatrix}i_{sa}\\i_{sb}\\i_{sc}\end{bmatrix} \; ; \quad \begin{bmatrix}u_{s\alpha}\\u_{s\beta}\end{bmatrix} = C_{23}\begin{bmatrix}u_{sa}\\u_{sb}\\u_{sc}\end{bmatrix} \; ;$$
$$\begin{bmatrix}\Psi_{s\alpha}\\\Psi_{s\beta}\end{bmatrix} = C_{23}\begin{bmatrix}\Psi_{sa}\\\Psi_{sb}\\\Psi_{sc}\end{bmatrix} \; ; \quad C_{23} = \frac{1}{\sqrt{6}}\begin{bmatrix}2 & -1 & -1\\0 & \sqrt{3} & -\sqrt{3}\end{bmatrix} \tag{24}$$

The zero-component is zero because there is no star-point connection, and therefore, it is omitted.
The rotor quantities are transformed to the stator-connected $\alpha\beta$-system by means of a rotation and they are referred to the stator by using

$$\begin{bmatrix}i_{C\alpha,k}\\i_{C\beta,k}\end{bmatrix} = C_s C_{r,k}\begin{bmatrix}i_{cd,k}\\i_{cq,k}\end{bmatrix} \; ; \quad \begin{bmatrix}\Psi_{C\alpha,k}\\\Psi_{C\beta,k}\end{bmatrix} = \frac{1}{C_s}C_{r,k}\begin{bmatrix}\Psi_{cd,k}\\\Psi_{cq,k}\end{bmatrix} \; ;$$
$$C_{r,k} = \begin{bmatrix}\cos(pk\theta) & -\sin(pk\theta)\\\sin(pk\theta) & \cos(pk\theta)\end{bmatrix} \; ; \tag{25}$$
$$C_s = \sqrt{\frac{2}{3}\frac{N_{c,k}}{N_{s,k}}\frac{r_c^{2kp}+r_s^{2kp}}{r_c^{kp}r_s^{kp}}}$$

The resulting voltage equations can be written as

$$\begin{cases}\begin{bmatrix}u_{s\alpha}\\u_{s\beta}\end{bmatrix} = \begin{bmatrix}e_{p\alpha}\\e_{p\beta}\end{bmatrix} + R_s\begin{bmatrix}i_{s\alpha}\\i_{s\beta}\end{bmatrix} + L_\sigma\frac{\mathrm{d}}{\mathrm{d}t}\begin{bmatrix}i_{s\alpha}\\i_{s\beta}\end{bmatrix} + \sum\limits_{k=1,5,7,11,..}^{\infty} L_k\frac{\mathrm{d}}{\mathrm{d}t}\begin{bmatrix}i_{s\alpha}+i_{C\alpha,k}\\i_{s\beta}+i_{C\beta,k}\end{bmatrix}\\ \begin{bmatrix}0\\0\end{bmatrix} = R_{C,k}\begin{bmatrix}i_{C\alpha,k}\\i_{C\beta,k}\end{bmatrix} + L_k\frac{\mathrm{d}}{\mathrm{d}t}\begin{bmatrix}i_{s\alpha}+i_{C\alpha,k}\\i_{s\beta}+i_{C\beta,k}\end{bmatrix} + nkp\Omega L_k\begin{bmatrix}i_{s\beta}+i_{C\beta,k}\\-i_{s\alpha}-i_{C\alpha,k}\end{bmatrix}\end{cases} \tag{26}$$

where

$$\begin{bmatrix}e_{p\alpha}\\e_{p\beta}\end{bmatrix} = \sum_{k=1,3,5,..}^{\infty}\hat{e}_{p,k}\begin{bmatrix}-\sin(kp\theta)\\\cos(kp\theta)\end{bmatrix} \tag{27}$$

$$\hat{e}_{p,k} = \sqrt{\frac{3}{2}}\frac{(r_m^{2kp}-r_r^{2kp})r_s^{kp}r_r}{(r_s^{2kp}-r_r^{2kp})r_m^{kp}}\frac{\pi}{2}\mu_0 l_s N_{s,k}\hat{M}_{p,k}\Omega \tag{28}$$

$$\Omega = \frac{\mathrm{d}\theta}{\mathrm{d}t} \tag{29}$$

$$L_\sigma = L_{s\sigma a} - M_{s\sigma ab} + \sum_{k=1,5,7,11,..}^{\infty}\frac{r_s^{2kp}-r_c^{2kp}}{r_s^{2kp}+r_c^{2kp}}\frac{3\mu_0\pi l_s N_{s,k}^2}{8kp} \tag{30}$$

$$L_k = \frac{(r_c^{2kp}+r_r^{2kp})r_s^{2kp}}{(r_c^{2kp}+r_s^{2kp})(r_s^{2kp}-r_r^{2kp})}\frac{3\mu_0\pi l_s N_{s,k}^2}{4kp} \tag{31}$$

$$R_{C,k} = \frac{6r_s^{2kp}r_c^{2kp}}{(r_c^{2kp}+r_s^{2kp})^2}\frac{\pi l_s \rho_c N_{s,k}^2}{4r_c\delta_c} \tag{32}$$

$$n = \begin{cases}1 & \text{for } k=1,7,13,..\\-1 & \text{for } k=5,11,17..\end{cases} \tag{33}$$

The equivalent circuit representing the α-component of this voltage equation is depicted in figure 3.

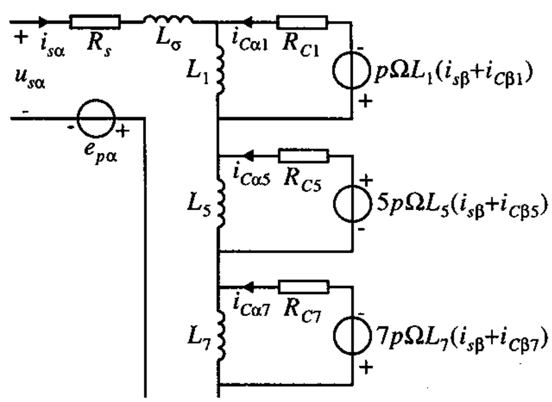

Figure 3: Equivalent circuit for the α-component of the voltage equation. The first, fifth, and seventh space harmonic are depicted; for the other space harmonics, the circuit can be extended in the same way.

4 LOCKED-ROTOR TESTS

The derived model is verified by comparing the calculated and the measured impedances of a machine with locked rotor. During the tests, a sinusoidal voltage is supplied to phases b and c, which are connected in series. The impedance calculated from (26) is

$$\underline{Z} = \frac{\hat{\underline{u}}_{sbc}}{\hat{\underline{i}}_{sb}} = 2\left(R_s + \mathrm{j}\omega L_\sigma + \sum_{k=1,5,7,11,..}^{\infty}\frac{\mathrm{j}\omega L_k R_{C,k}}{R_{C,k}+\mathrm{j}\omega L_k}\right)$$
$$R = \mathrm{Re}(\underline{Z}) \; ; \quad L = \frac{1}{\omega}\mathrm{Im}(\underline{Z}) \tag{34}$$

The resistance and the inductance of the machine are determined from the measured voltage U_{sbc}, the current I_{sb}, and the dissipation P in the machine as

$$R = \frac{P}{I_{sb}^2} \; ; \qquad L = \frac{1}{\omega}\sqrt{\left(\frac{U_{sbc}}{I_{sb}}\right)^2 - R^2} \tag{35}$$

The results are depicted in figure 4. The differences between the measured and the calculated resistance above 1000 Hz is caused by iron losses [6]. The influence of the higher space harmonics on the test results is so small that the tests verify nor refute the model. For the fundamental space harmonic, the correlation is good and the model is verified.

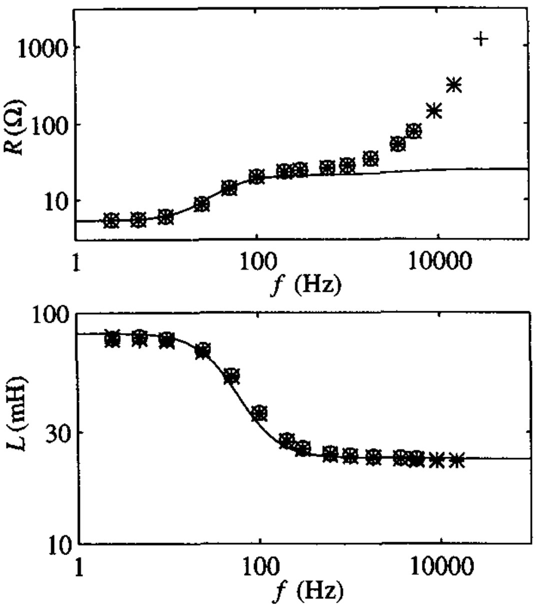

Figure 4: Measured (+: I_{sb}=0.1 A, ×: I_{sb}=0.2 A, ∗: I_{sb}=0.5 A, ○: I_{sb}=1 A, ·: I_{sb}=2 A) and calculated (—) resistance and inductance during the locked-rotor tests.

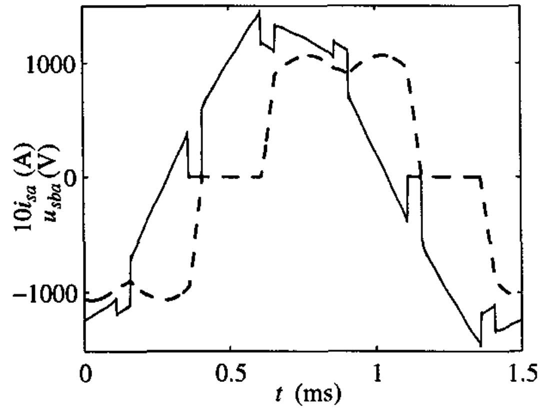

Figure 5: Calculated voltage (—) and current (--) waveforms.

5 RECTIFIER LOADED MACHINE

The voltage and current waveforms of a 120 kW 20000 rpm rectifier-loaded permanent-magnet machine with shielding cylinder are calculated with the calculation method described in [9]. They are depicted in figure 5. The losses in the shielding cylinder with a thickness of 0.5 mm are calculated as 362 W.

6 CONCLUSIONS

The paper introduces a model of a permanent-magnet machine with shielding cylinder based on the two-dimensional calculation of the magnetic field. This model is suitable for calculation of the losses in the shielding cylinder and the voltage and current waveforms. Because the model is analytic, it gives insight into the relations between dimensions and parameters of the machine, which is important when the design is optimized.

REFERENCES

1. J.L.F. van der Veen, L.J.J. Offringa, A.J.A. Vandenput, 1997, "Minimizing rotor losses in high-speed high-power permanent magnet synchronous generators with rectifier load", IEE Proceedings - Electric Power Applications, vol. 144, pp. 331-337.
2. S.M. Abu Sharkh, M.R. Harris, N. Taghizadeh Irenji, 1997, "Calculation of rotor eddy-current loss in high-speed PM alternators", Proceedings of the Eighth International Conference on Electrical Machines and Drives, pp. 170-174.
3. N. Boules, 1981, "Impact of slot harmonics on losses of high-speed permanent magnet machines with a magnet retaining ring", Electric Machines and Electromechanics, vol. 6, pp. 527-539.
4. M. Poloujadoff, 1980, "The theory of linear induction machinery", Clarendon Press, Oxford.
5. H. Polinder, M.J. Hoeijmakers, 1997, "Analytic calculation of the magnetic field in PM machines", Conference Record of the IEEE Industry Applications Society Annual Meeting, pp. 35-41.
6. H. Polinder, 1998, "On the losses in a high-speed permanent-magnet generator with rectifier - with special attention to the effect of a damper cylinder". PhD Dissertation, Delft University of Technology, EburonP&L, Delft.
7. H.A. Haus, J.R. Melcher, 1989, "Electromagnetic fields and energy". Prentice Hall, Englewood Cliffs, New Jersey.
8. G.R. Slemon, 1992, 'Electric machines and drives', Addison-Wiley, Reading, Massachusetts.
9. H. Polinder, M.J. Hoeijmakers, L.J.J. Offringa, W. Deleroi, 1996, "Harmonic analysis of a PM machine with rectifier", Proceedings of the Sixth International Conference on Electrical Machines, vol. 2, pp. 63-68.